Winter Persistence Barrier of Sea Surface Temperature in the Northern Tropical Atlantic Associated with ENSO

RUIQIANG DING AND JIANPING LI

State Key Laboratory of Numerical Modeling for Atmospheric Sciences and Geophysical Fluid Dynamics (LASG), Institute of Atmospheric Physics, Chinese Academy of Sciences, Beijing, China

(Manuscript received 13 April 2010, in final form 29 January 2011)

ABSTRACT

This study investigates the persistence characteristics of the sea surface temperature anomaly (SSTA) in the northern tropical Atlantic (NTA). It is found that a persistence barrier exists around December and January. This winter persistence barrier (WPB) is prominent during the mature phase of strong ENSO events but becomes indistinct during weak ENSO and normal (non-ENSO) events. During strong El Niño events, the NTA SSTA shows a reversal in sign and a rapid warming during December and January. It is possible that this SSTA sign reversal reduces the persistence, leading to the occurrence of the NTA WPB. The present analyses indicate a dynamic relationship among the Pacific ENSO, the NTA SSTA, and the NTA WPB on a quasi-biennial time scale: a strong El Niño event is usually preceded by a strong La Niña event, which leads to a sign reversal of the NTA SSTA in winter as a delayed response to ENSO, finally resulting in the NTA WPB. Analyses also suggest that the NTA WPB is affected by the North Atlantic Oscillation (NAO). The NAO enhances the persistence of the NTA SSTA during winter, tending to weaken the NTA WPB.

1. Introduction

The El Niño–Southern Oscillation, originating in the tropical Pacific, has a widespread effect on the global climate system. Considerable research effort has been devoted to predicting ENSO at seasonal lead times using dynamical and statistical models, both of which have met with great success (e.g., Latif et al. 1998; Barnston et al. 1999; Jin et al. 2008). However, most models developed to predict ENSO suffer from a rapid decrease in forecast skill in the boreal spring months of March–May, reflecting the existence of a spring persistence barrier (SPB) in ENSO anomalies (Webster and Yang 1992). The causes of this phenomenon are not yet fully understood. Some studies have suggested that it may reflect the relatively weak ocean–atmosphere coupling over the Pacific during boreal spring (Zebiak and Cane 1987; Blumenthal 1991; Goswami and Shukla 1991). More recent studies have emphasized the phase locking of ENSO to the annual cycle (Torrence and Webster 1998; An and Wang 2001) and the biennial component of ENSO (Clarke and Van Gorder 1999; Yu 2005).

In addition to the well-known SPB in the tropical central-eastern Pacific, persistence barriers also occur in other ocean areas during seasons other than spring. Wajsowicz (2005) reported a winter persistence barrier (WPB) of the sea surface temperature anomaly (SSTA) in the southeastern tropical Indian Ocean (STIO), associated with strong seasonal phase locking of the Indian Ocean dipole (IOD) (Saji et al. 1999; Luo et al. 2007). In the extratropical North Pacific and North Atlantic, a persistence barrier of the SSTA exists around July–September (Namias and Born 1970, 1974; Deser et al. 2003; Ding and Li 2009; Zhao and Li 2010), related to diminished wind stress and vertical mixing in ocean surface layers during the boreal summer. Chen et al. (2007) reported a fall persistence barrier (FPB) of the SSTA in the South China Sea (SCS), which is well recognized during the developing phase of strong ENSO cases but becomes vague in weak ENSO and non-ENSO cases. Zhao and Li (2009) showed that the persistence barrier of SSTA exists not only in the SCS but also in the vicinity of Indonesia. The SCS barrier occurs around October and November, while the barrier in the Indonesia region occurs around November and

Corresponding author address: Dr. Jianping Li, State Key Laboratory of Numerical Modeling for Atmospheric Sciences and Geophysical Fluid Dynamics, Institute of Atmospheric Physics, Chinese Academy of Sciences, Beijing 10029, China.
E-mail: ljp@lasg.iap.ac.cn

DOI: 10.1175/2011JCLI3784.1

December. These persistence barriers may strongly influence the skill of SST predictions when predictions are made across the season in which the barriers occur.

SSTA variability in the tropical Atlantic (TA) is typically weaker than ENSO and is generally given little attention in global seasonal forecast systems. Yet SSTA variability in the TA is by no means negligible and could have a strong influence on regional climate. A number of well-known climatic phenomena in the TA sector (e.g., rainfall over northeast Brazil and sub-Saharan drought) are closely linked to SSTA variability in the TA (Moura and Shukla 1981; Folland et al. 1986; Xie and Carton 2004; Taschetto and Wainer 2008). Given the importance of the TA SSTA in terms of its influence on regional climate, it is of interest to investigate the seasonal dependence of the SSTA persistence in the TA. Recent studies have suggested that the ENSO-related SSTA in the tropical eastern Pacific has a significant remote influence on SSTA variability in the TA sector (e.g., Enfield and Mayer 1997; Penland and Matrosova 1998; Latif and Grötzner 2000; Saravanan and Chang 2000; Elliott et al. 2001; Mo and Häkkinen 2001; Chang et al. 2003; Huang 2004). The main region affected by ENSO is the northern tropical Atlantic (NTA), where significant warming occurs approximately 4–5 months after the mature phase of Pacific warm events (Enfield 1996; Enfield and Mayer 1997).

The mechanisms responsible for the link between ENSO and the NTA variability have been extensively studied (e.g., Nobre and Shukla 1996; Saravanan and Chang 2000; Sutton et al. 2000; Wang 2002, 2004; Handoh et al. 2006). There are at least two mechanisms via which ENSO may influence the NTA region: 1) changes to the tropical Walker and Hadley circulations and associated patterns of deep convection (Bjerknes 1969; Oort and Rasmusson 1970) and 2) tropical–extratropical interaction via the Pacific–North American (PNA) teleconnection pattern (Wallace and Gutzler 1981). Some controversy remains regarding which of the above mechanisms plays a major role in the link between ENSO and NTA variability (Chang et al. 2006). Handoh et al. (2006) emphasized the important role of tropical–extratropical interaction in inducing anomalous SST over the NTA. Their analysis suggests that the ENSO-associated NTA SSTA is forced by an extratropical PNA-like wave train emanating from the Pacific, rather than by a change in the Walker circulation. Nobre and Shukla (1996) also found that off-equatorial TA (warm or cold) events are unlikely to be induced by a change in the Walker circulation. However, the modeling study of Saravanan and Chang (2000) showed that the teleconnection between the eastern tropical Pacific and the NTA is explained by an anomalous Walker circulation and that there is no need to invoke any extratropical teleconnection mechanism such as the PNA pattern. Wang (2002, 2004) suggested that the Pacific El Niño can affect the NTA through the Walker and Hadley circulations, favoring NTA warming in the subsequent spring of Pacific El Niño years. Sutton et al. (2000) speculated that the two mechanisms compete in influencing the NTA variability, with different regions of the NTA being dominated by different mechanisms: north of 7.5°N, the PNA pattern dominates; south of 7.5°N, changes in the Walker and Hadley circulations dominate.

In fact, both mechanisms generate a similar local response of the NTA to ENSO: changes in surface winds induce changes in surface heat fluxes that in turn generate anomalous SST (Carton et al. 1996; Nobre and Shukla 1996; Chang et al. 1997; Saravanan and Chang 2000; Foltz and McPhaden 2006). Bates (2008) reported that tropical Atlantic variability is initiated by atmospheric perturbations acting on the easterly trade winds, the presence of which is necessary to trigger anomalies in various regions of the TA (including the NTA). Specifically, a perturbation of the northeast trade winds results in the SSTA in the NTA region, which is generated by influences such as ENSO, the North Atlantic Oscillation (NAO), and the annual cycle (Bates 2010).

ENSO forces a delayed (relative to the mature phase of ENSO) warming of the NTA SST via weakening of the northeasterly trade winds and consequent reduction in surface heat fluxes. This delayed warming forces a northward displacement of the Atlantic intertropical convergence zone (ITCZ), resulting in increased precipitation over the Caribbean and reduced precipitation over northeast Brazil during the boreal spring following the mature phase of ENSO (Nobre and Shukla 1996; Giannini et al. 2001a). In this way, the ENSO information in winter is passed to the following TA spring rainfall via the NTA SSTA. The aforementioned studies have shown a close linkage between ENSO and the NTA SSTA. However, a detailed analysis of how ENSO influences the persistence of the NTA SSTA is still lacking. The evolutionary features of the NTA SSTA associated with different ENSO cases may be different; therefore, it is interesting to investigate the persistence features of the NTA SSTA associated with different ENSO cases. A better understanding of the persistence features of the NTA SSTA would result in improved climate predictions for the TA. The dynamic relationships that exist between the NTA SSTA and ENSO give rise to two interesting questions: Does the ENSO remote influence lead to a persistence barrier in the NTA SSTA? If so, what are possible mechanisms responsible for the occurrence of this barrier? The objective of the present study is to answer these two questions. The present findings are expected to be helpful in studying TA climate variability and in improving predictions of the TA SSTA.

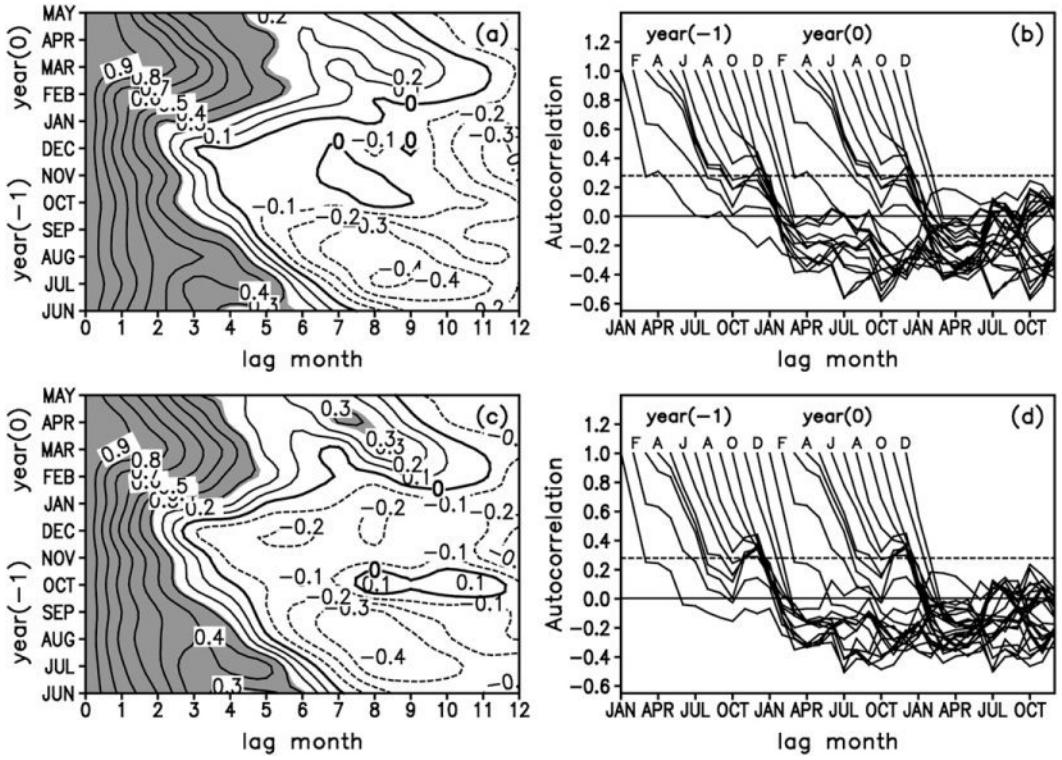

FIG. 1. (a) Autocorrelations of the area-averaged SSTA over the NTA from the ERSST dataset as a function of starting calendar month and lag time for the period 1950–2002. Contour interval is 0.1; the zero contour is highlighted. Autocorrelations significant at the 0.05 level (≥0.27) are shaded. (b) As in (a), but for autocorrelation curves of the NTA SSTA. Each curve has been shifted to align the starting month (shown at the top, where FAJAOD is February, April, June, August, October, December) with the corresponding lag month (x axis). The horizontal dashed line indicates the 0.05 significance level. (c) As in (a), but (b) for the NTA SSTA from the HadISST dataset and (d) for the NTA SSTA from the HadISST dataset.

2. Data and methodology

The basic SST dataset used in this study is version 2 of monthly NOAA Extended Reconstructed SST (ERSST) data on a 2° × 2° spatial grid for the period 1950–2002 (Smith and Reynolds 2004). The results obtained from ERSST are verified using the Hadley Center Sea Ice and SST dataset (HadISST) on a 1° × 1° spatial grid for the same period. For the analyses of atmospheric circulation, 2.5° × 2.5° National Centers for Environmental Prediction–National Center for Atmospheric Research reanalysis data (1950–2002) (Kalnay et al. 1996) are employed. Prior to analysis, the area-averaged SST data were obtained over the NTA (5°–15°N, 20°–60°W). To obtain the NTA SSTA, the climatological mean annual cycle is removed from the area-averaged NTA SST time series, which are then passed through a 7-yr high-pass Gaussian filter. In this way, the annual cycle and decadal components are removed from the NTA SST. Autocorrelation analysis was used to measure the persistence of the NTA SSTA, which is defined as the correlation between the time series of the starting calendar month (January–December) and the time series of a succeeding lag month in a period of given duration.

3. Persistence characteristics of the NTA SST

Figure 1a shows the autocorrelations of the NTA SSTA from the ERSST dataset for the entire analysis period (1950–2002). In Fig. 1a, the reference year [year (0)] is assigned as each year from 1951 to 2002, while the previous year [year (−1)] is assigned as each year from 1950 to 2001. An annual cycle, from June of year (−1) to May of year (0), is considered when calculating the autocorrelations. Autocorrelations significant at the 0.05 level (≥0.27) are shaded in the figure. The time taken for autocorrelations to attain the 0.05 significance level can be regarded as a measure of SST persistence starting from that month. Figure 1b is similar to plots in Webster and Yang (1992), which contains the same information as Fig. 1a but clearly shows the occurrence time of a persistence barrier. According to Webster and Yang (1992), the persistence barrier refers to a phenomenon of autocorrelations showing

TABLE 1. Member years of strong ENSO, weak ENSO, and normal (non-ENSO) cases.

Strong ENSO	El Niño	1958, 1966, 1973, 1983, 1987, 1992, 1995, 1998
	La Niña	1956, 1968, 1971, 1974, 1976, 1985, 1989, 1999, 2000
Weak ENSO	El Niño	1964, 1969, 1970, 1977, 1978, 1980, 1988, 1993
	La Niña	1951, 1955, 1963, 1965, 1972, 1975, 1996, 1997
Normal	Positive	1952, 1953, 1954, 1959, 1979, 1982, 1990, 1991, 1994
	Negative	1957, 1960, 1961, 1962, 1967, 1981, 1984, 1986, 2001, 2002

a rapid and significant decrease (autocorrelation reduces to half its value) from one month to the next, regardless of the starting month.

Figure 1a shows that the NTA SSTA has the high persistence in the starting months of June and July in year (−1) (the coefficients fall below the 0.05 significance level after about 6 months). From June to December of year (−1), the persistence of the NTA SSTA shows a continuous drop, with a minimum occurring from December to January. From January to February of year (0), the persistence of the NTA SSTA shows a sharp rise. These results clearly demonstrate that the persistence of the NTA SSTA reaches a minimum in December and January (the coefficients fall below the 0.05 significance level after about 2 months). From Fig. 1b, autocorrelations of the NTA SSTA show a rapid decrease in December–January, regardless of the starting month. Although autocorrelations starting from February to May lose statistical significance after 4–5 months, they still experience a significant decrease from a positive value to near zero in December–January after significance is lost. Moreover, the autocorrelation value in December is about half or less of that in January for most of the starting months (Table not shown). According to the Webster and Yang (1992) criterion, there is a WPB in the NTA SSTA. Autocorrelations calculated from the Met Office Hadley Centre Sea Ice and SST (HadISST) dataset (Figs. 1c and 1d) are very similar to those shown in Figs. 1a and 1b, confirming the results obtained from the ERSST dataset.

To investigate the relationship between ENSO and the NTA WPB, ENSO cases are classified into three types according to the intensity of the winter [December–February (DJF)] SSTA in the Niño-3 region. The year assigned to each winter is that including January and February. The assigned year and the previous year are referred to as year (0) and year (−1), respectively. A strong (weak, normal) ENSO case is defined as a year in which the winter Niño-3 SSTA has an intensity greater than 1.0 (0.5–1.0, smaller than 0.5) standard deviation (SD) of its 1950–2002 time series (Table 1). Figure 2 examines the persistence characteristics of the NTA SSTA for these three cases. For strong ENSO cases (Fig. 2a), the NTA SSTA shows a minimum persistence during December and January, while it shows a relatively high persistence for other starting months. Autocorrelations of the NTA SSTA for strong ENSO cases, regardless of the starting month, decrease quickly from positive values to negative values in December–January (Fig. 2b). Clearly, there exists a well-defined WPB in the NTA SSTA for strong ENSO cases. For weak ENSO (Fig. 2c) and normal cases (Fig. 2e), a two-humped structure is present with longer persistence in around July–August and March–April (compared with other starting months). The NTA SSTA shows relatively low persistence from September to February during normal cases, while it shows a relatively low persistence around February, May, and October during weak ENSO cases. In both cases, the minimum persistence does not occur in December or January; autocorrelations starting from January to October do not show a rapid decrease in December–January (Figs. 2d,f). Although the sign structure appears similar during strong ENSO and normal cases (Figs. 2a,c), it will be shown later that the evolutionary features of the NTA SSTA during normal cases are completely different from those during strong ENSO cases (see Fig. 7 in Section 4). The WPB of the NTA SSTA is absent in weak ENSO and normal cases.

To further investigate the influence of ENSO on the persistence of the NTA SSTA, the ENSO signal is removed from the original NTA SSTA by a multiple linear regression method, yielding the residual NTA SSTA. Although it is impossible to remove all ENSO aspects from the original NTA SSTA by the multiple linear regression method, linear removal of the ENSO signal can reduce the influence of ENSO on the persistence of the NTA SSTA to a certain extent. Figure 3 shows the autocorrelations of the residual NTA SSTA for the entire analysis period 1950–2002. With removal of the ENSO signal, the persistence characteristics of the NTA SSTA show a prominent change, and the WPB phenomenon becomes less significant than that obtained from the original NTA SSTA, as shown in Fig. 1. The difference between Fig. 3a and Fig. 1a shows that, with the ENSO signal removed, autocorrelations starting from November to January are largely enhanced for lag times of 1–4 months; those starting from July to September are slightly enhanced for lag times of 1–4 months (a marked increase for lag times greater than 5 months is due to the negative correlation not being as strong in Fig. 3a as in Fig. 1a, not due to the NTA SSTA persisting longer) (Fig. 4). On the

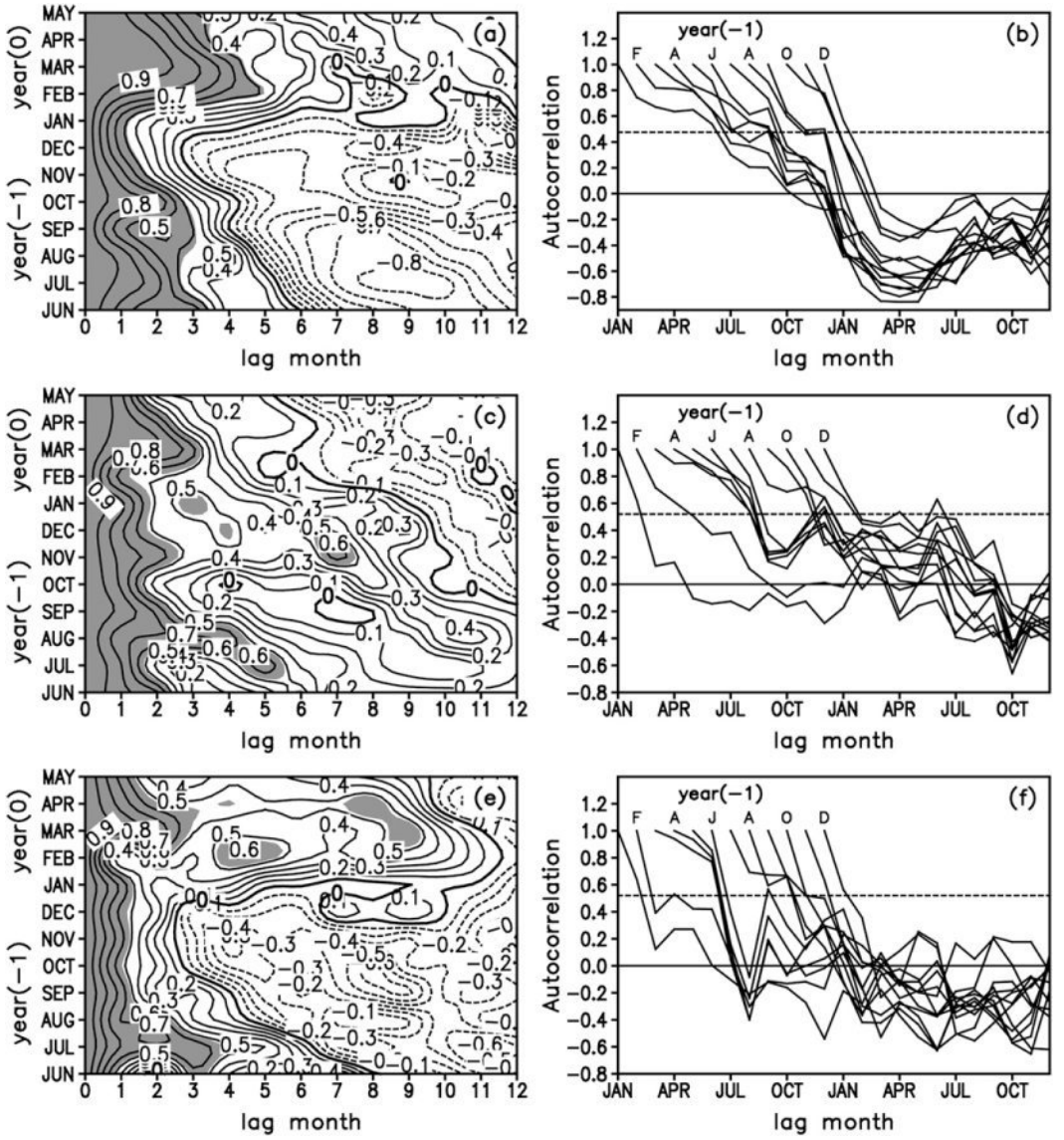

FIG. 2. Autocorrelations of (left) the area-averaged SSTA over the NTA as a function of starting calendar month and lag time for (a) strong ENSO, (c) weak ENSO, and (e) normal cases and (right) of the NTA SSTA as a function of starting calendar month and lag time for (b) strong ENSO, (d) weak ENSO, and (f) normal cases. In (a),(c),(e) the zero contour is highlighted; autocorrelations significant at the 0.05 level are shaded. In (b),(d),(f) the starting months are in year (−1) (i.e., prior to the winter mature phase of ENSO); the horizontal dashed line indicates the 0.05 significance level.

contrary, autocorrelations starting from February to June are remarkably reduced for most lag months after the ENSO signal is removed. We conclude from these results that ENSO may cause the NTA SSTA to persist longer in February–June and may suppress the persistence in November–January and July–September. With the increased persistence in November–January and the decreased persistence in February–June, the minimum persistence of the NTA SSTA does not occur around December and January after the ENSO signal is removed, thereby leading to an indistinct WPB. These results support the proposal that the occurrence of the WPB of the NTA SSTA is closely connected to ENSO. In addition, we note that the persistence of the residual NTA SSTA in Fig. 3a for the starting months of July–September is relatively long and that it shows a rapid decrease from September to October. This phenomenon is also prominent in the weak ENSO (Fig. 2c) and normal cases (Fig. 2e). It is speculated that a September–October persistence barrier of the NTA SSTA may exist in the absence of ENSO, while ENSO tends

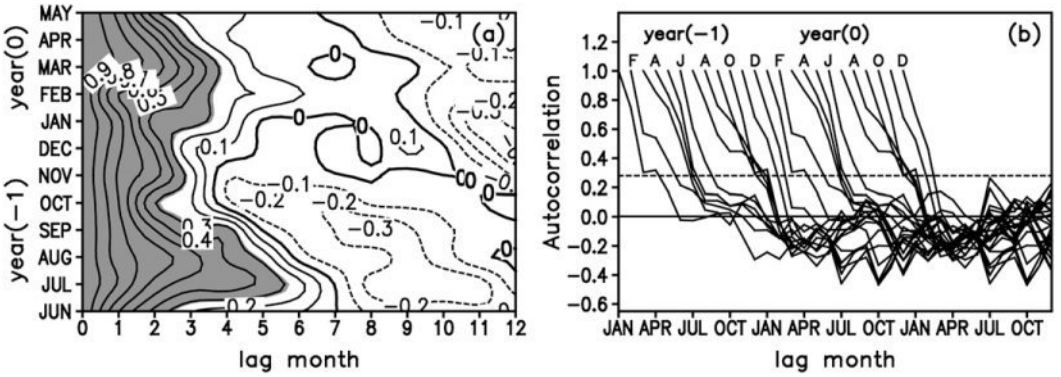

FIG. 3. As in Fig. 1a and Fig. 1b, respectively, but for the residual NTA SSTA obtained by removing the ENSO signal from the original NTA SSTA. The lead–lag correlations with Niño-3 SSTA show that the NTA SSTA has significant correlations with the Niño-3 SSTA with lead times of 3–5 months. Therefore, the ENSO signal in the NTA SSTA is obtained by regressing the NTA SSTA upon the Niño-3 SSTA with lead times of 3–5 months.

to remove this barrier. The study of such a September–October barrier is beyond the objective of the present paper, but is a good topic for future research.

Is the WPB robust in the NTA region? According to Enfield and Mayer (1997), ENSO exerts a remote influence over an extensive region of the NTA from northwest Africa to the Caribbean Sea. Autocorrelations of the area-averaged SST over a larger region of the NTA (5°–20°N, 10°–70°W) including the coast of northwest Africa and the eastern part of the Caribbean Sea) were computed for all cases and strong ENSO cases. Their persistence features (not shown) are relatively consistent with those obtained using the original SST index. The results indicate that the WPB is not sensitive to the analysis domain and is robust in the NTA region.

4. Evolution of the NTA SSTA associated with ENSO

Previous studies have discussed the evolution of the NTA SSTA pattern and potential influences (including ENSO) in different seasons (e.g., Huang and Shukla 2005; Handoh et al. 2006; Bates 2008). However, few studies have performed detailed investigations of the evolutionary features of the NTA SSTA associated with different ENSO cases, which is necessary to identify the mechanisms that induce the NTA WPB. In this section, we compare in detail the evolutionary features of the NTA SSTA among different ENSO cases, with the aim of identifying the mechanisms that induce the NTA WPB.

Figure 5 shows composite difference patterns of the SSTA (strong El Niño minus strong La Niña) during the developing, mature, and decaying phases of ENSO [October of year (−1) to May of year (0)]. In the tropical Pacific, the SSTA patterns reflect the dominant features of El Niño evolution. The central and eastern equatorial Pacific is dominated by strong and sustained warming, while the tropical western Pacific shows a minor cooling. The El Niño reaches its mature phase during December and January when the maximum warming occurs in the eastern equatorial Pacific. After February, the significant warming in the eastern equatorial Pacific begins to weaken and El Niño enters its decaying stage. The NTA shows a different pattern of SSTA change. Before December, the NTA is dominated by weak negative SSTA. An anomalous warming in the NTA begins to emerge in January and becomes significant in February. It extends southward to cover the entire NTA in March and then persist for several months. The maximum warming center is located off the coast of northwest Africa, stretching farther westward into the central NTA from March to May. In general, the

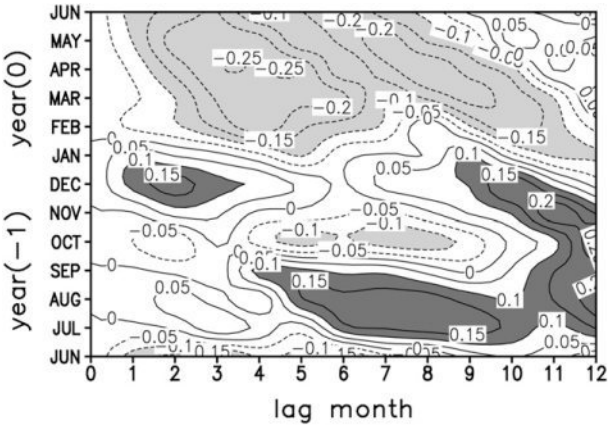

FIG. 4. Difference between autocorrelations obtained from the residual NTA SSTA (as in Fig. 3a) and those obtained from the original NTA SSTA (as in Fig. 1a). Contour interval is 0.05; the difference greater than 0.1 or less than −0.1 is shaded.

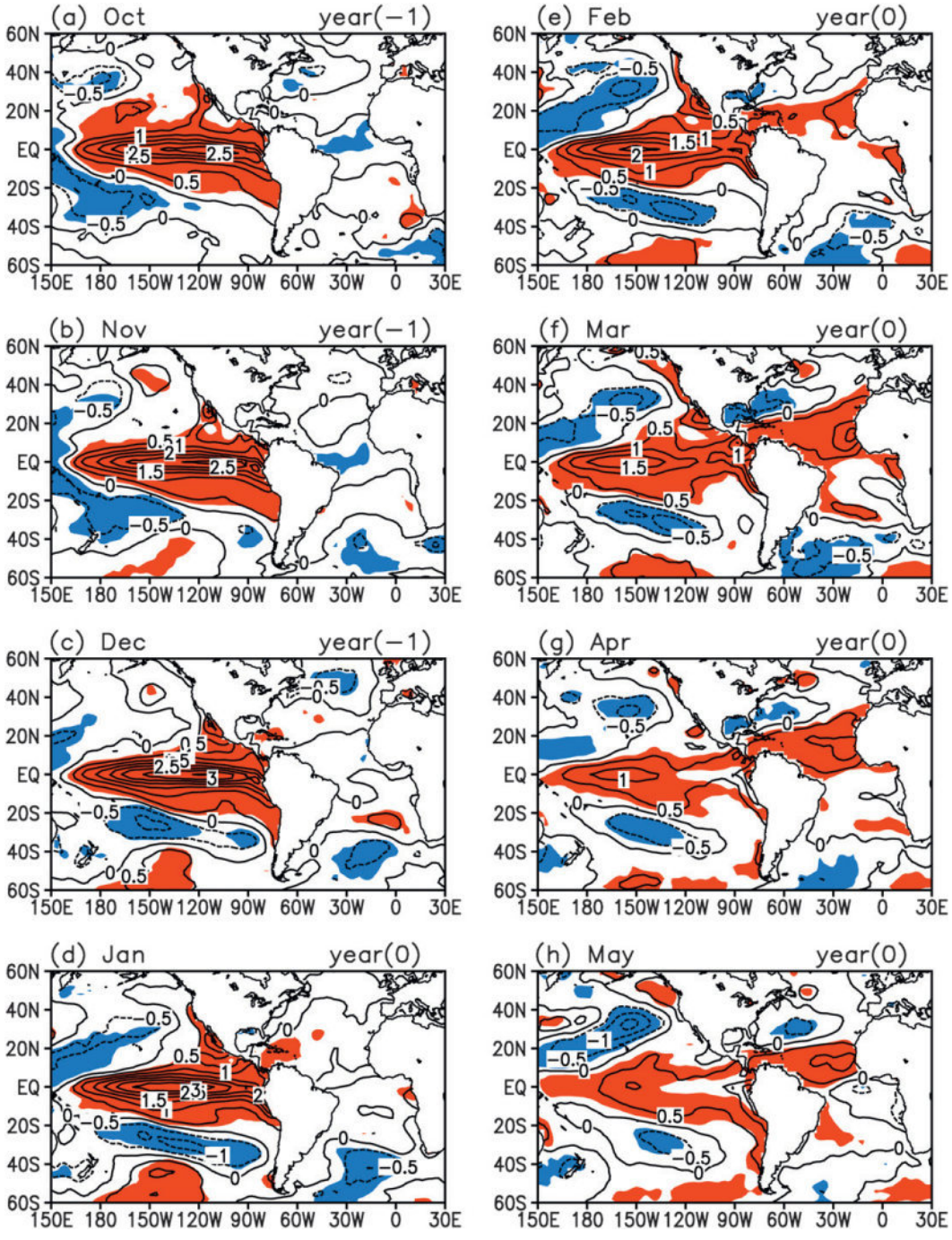

FIG. 5. Composite SSTA difference for strong ENSO cases (El Niño minus La Niña) during the developing, mature and decaying phases of ENSO [October of year (−1) to May of year (0)]. Contour interval is 0.5°C; anomalies significant at the 0.05 level are shaded.

evolutions of the NTA SSTA associated with a strong ENSO are similar to those described in previous studies (e.g., Enfield and Mayer 1997; Saravanan and Chang 2000; Mo and Häkkinen 2001; Chang et al. 2003; Huang 2004; Handoh et al. 2006).

The area-averaged SSTA over the NTA demonstrates more clearly the evolutionary features of the ENSO-related SSTA in the NTA (Fig. 6). The warm El Niño events (or cold La Niña events) lead by approximately 3–5 months a warm (or cold) signature in the NTA SSTA.

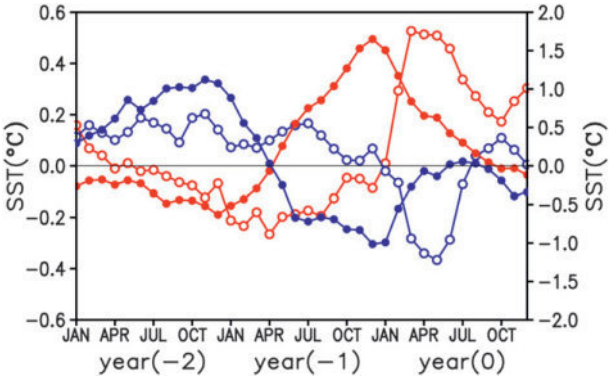

FIG. 6. (left, *y* axis) Composite of the area-averaged SSTA over the NTA for strong El Niño events (red line with open circle) and strong La Niña events (blue line with open circle) from January of year (−2) to December of year (0). (right, *y* axis) Composite of the area-averaged SSTA over the Niño-3 region for strong El Niño events (red line with closed circle) and strong La Niña events (blue line with closed circle).

The NTA SSTA shows a reversal in sign from negative to positive (or from positive to negative) during December and January. The NTA WPB coincides with this sign reversal in the NTA SSTA during winter, indicating a close link between the two phenomena. The SSTA sign reversal implies a rapid decrease in the SSTA persistence, which is favorable for the occurrence of a persistence barrier. The SSTA sign reversal occurs in the tropical eastern Pacific during spring (Webster and Yang 1992) and in the SCS during fall (Chen et al. 2007), consistent with the seasons during which the persistence barriers occur.

The NTA SSTA shows a sign reversal from negative to positive (or from positive to negative) in winter (December–January) during strong ENSO cases. The NTA WPB is closely related to this sign reversal of SSTA in boreal winter. It is important to also consider the evolution of the NTA SSTA during weak ENSO and normal cases. We compare the evolutionary features of SSTAs among different ENSO cases in terms of their composite longitude–time patterns averaged over 5°–15°N (Fig. 7). The composite patterns are obtained from the differences between El Niño and La Niña cases or between positive and negative normal cases. For strong ENSO cases, the NTA SST changes from negative anomalies in fall of year (−1) to positive anomalies in spring of year (0) (Fig. 7a). A phase reversal occurs during winter (December–January). However, for weak ENSO cases, although positive SSTA occurs in spring of year (0), it is also positive in fall of year (−1) (Fig. 7b). Therefore, no phase reversal of SSTA occurs during weak ENSO cases, leading to an indiscernible WPB. During normal cases, the WPB is unlikely to happen owing to a disordered evolution pattern and low intensity of the NTA SSTA (Fig. 7c).

During strong ENSO cases, the sea level pressure (SLP) anomaly undergoes a sign reversal between fall of year (−1) and spring of year (0) (Fig. 7d). In winter, the rapid warming of the NTA SST is associated with a rapid drop in SLP. These relationships suggest that the sign reversal of the NTA SSTA that occurs between fall and the following spring during strong ENSO cases is closely connected with rapid changes in the atmospheric circulation over the NTA region. As noted in previous studies (e.g., Nobre and Shukla 1996; Saravanan and Chang 2000; Sutton et al. 2000; Wang 2002, 2004; Handoh et al. 2006), rapid changes in the SLP over the NTA region appear to be a passive response to remote ENSO forcing, mainly via an anomalous Walker circulation or the PNA teleconnection, which in turn induce SST anomalies over the NTA through changes in surface winds and surface heat fluxes. The present study mainly discusses how ENSO influences the persistence of the NTA SSTA. The relative importance of the two mechanisms regarding the link between ENSO and the warming in the NTA is not assessed in this study; further research is necessary in this regard.

5. The NTA WPB and the quasi-biennial oscillation

It is clear that El Niño forces a delayed (relative to the mature phase of El Niño) warming of the NTA SST. However, the NTA SSTA undergoes a sign reversal between the periods before and after the occurrence of the WPB. It remains unclear why the negative NTA SSTA occurs before the occurrence of the WPB. The quasi-biennial component has been observed previously in ENSO variability (Rasmusson et al. 1990). El Niño events are often preceded or followed by La Niña events. Figure 6 shows that warm El Niño events are preceded by La Niña events. The negative NTA SSTA lags, by approximately 3 months, a cool signature in the eastern equatorial Pacific. Therefore, the negative NTA SSTA before the occurrence of the WPB could be caused by La Niña events preceded by strong El Niño events. The SSTA sign reversal from La Niña events to El Niño events occurs in spring, consistent with the SPB phenomenon in the tropical eastern Pacific. As a delayed response to ENSO, the SSTA sign reversal in the NTA occurs in winter, leading to a WPB. In this sense, the Pacific SPB is followed by the NTA WPB.

Power spectrum analysis reveals that interannual variation of the NTA SSTA shows an obvious quasi-biennial component with a period of about 2–3 years (Fig. 8). The evolution of the NTA SSTA associated with ENSO suggests that the quasi-biennial signal of the NTA SSTA is likely influenced by ENSO. Figure 9a shows the lead–lag correlations between the NTA and Niño-3 SSTAs. These correlations show an evident quasi-biennial oscillation

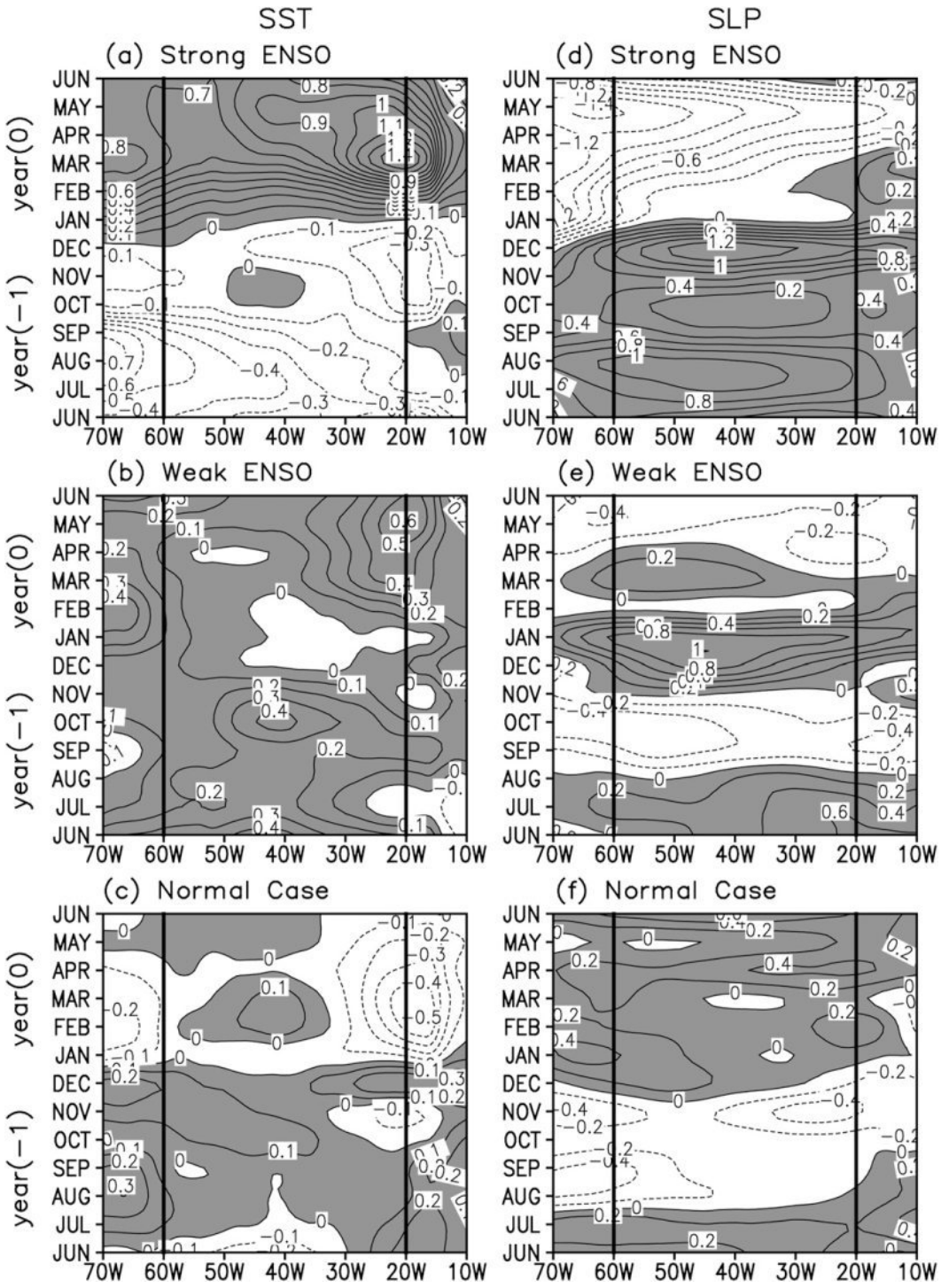

FIG. 7. Composite longitude–time patterns of SST–SLP difference anomalies averaged over 5°–15°N for (a),(d) strong ENSO (El Niño minus La Niña); (b),(e) weak ENSO (El Niño minus La Niña); and (c),(f) normal (positive minus negative) cases. Contour intervals are 0.1°C for SSTA and 0.2 mb for SLP anomaly; positive values are shaded. The analyzed NTA region is bounded by two thick vertical lines.

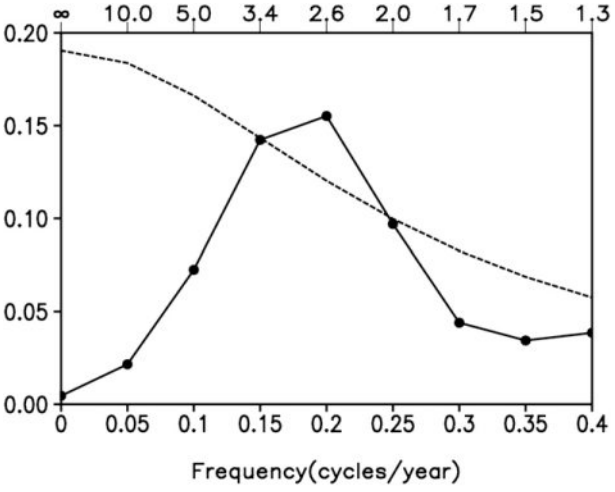

FIG. 8. Power spectrum (dotted solid line) of the monthly NTA SSTA time series for the period 1950–2002. The dashed line shows the 0.05 confidence upper limit of red noise spectrum.

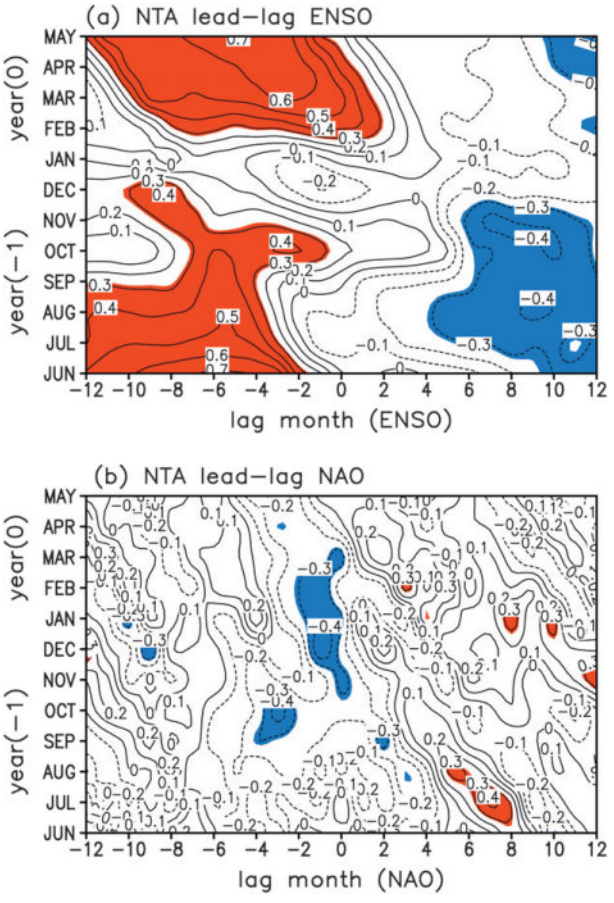

FIG. 9. (a) Lead–lag correlations between the area-averaged SSTAs over the NTA and the Niño-3 region for the period 1950–2002; (b) lead–lag correlations between the area-averaged SSTA over the NTA and the NAO index. The NTA SSTA from June of year (−1) to May of year (0) is used as the reference to compute the lead–lag correlation coefficients. Contour interval is 0.1; correlations significant at the 0.05 level are shaded.

(QBO) relationship throughout the year, except during winter months (December and January) when the NTA SSTA has a weak lead–lag correlation with ENSO.

Clarke and Van Gorder (1999) reported that the biennial oscillation embedded in the ENSO index might be responsible for the SPB in the eastern equatorial Pacific, which is phase locked to the calendar year. The quasi-biennial oscillation of the NTA SSTA also tends to be locked to the calendar year, with ENSO peaking in winter and the NTA SSTA peaking in the following spring (Fig. 6). These findings lead us to speculate that the NTA WPB might result from the quasi-biennial signal of the NTA SSTA, which is closely linked to ENSO. As shown in Fig. 7, the NTA WPB is well developed when the quasi-biennial variability of the NTA SSTA is prominent during strong ENSO cases. In contrast, the NTA WPB is poorly developed when the quasi-biennial variability of the NTA SSTA becomes indistinct during weak ENSO and normal cases. These results indicate the possible existence of a systematic relationship between the WPB, the NTA SST, and the quasi-biennial component of ENSO as follows: a strong El Niño event is usually preceded by a strong La Niña event, which leads to a sign reversal of the NTA SSTA in winter as a delayed response to ENSO, ultimately resulting in the NTA WPB. It is necessary to further examine the dynamic relationships among these phenomena and to consider the implications of these relationships in terms of improving predictions of the NTA SSTA and ENSO.

6. Influences of the NAO on the NTA WPB

In addition to the influence of ENSO, the SSTA over the NTA area is moderated by atmospheric circulation and heat flux anomalies related to the NAO. The heat flux anomalies associated with the NAO can enhance or diminish the impact of ENSO, depending on the NAO phase (e.g., Grötzner et al. 1998; Giannini et al. 2001b; Czaja et al. 2002). It has been demonstrated that atmospheric anomalies associated with NAO produce tripolelike SSTA in the North Atlantic (Deser and Timlin 1997; Marshall et al. 2001; Pan 2005). As the tropical Atlantic signature of the NAO-forced SST tripole in the North Atlantic, the NTA SST variability is also modulated by the NAO. This leads us to question the influence of NAO on the NTA WPB. The NAO index (NAOI) used in this study is defined as the difference in the normalized monthly SLP zonal-averaged over the North Atlantic sector between 35° and 65°N from 80°W to 30°E (Li and Wang 2003). According to the winter (DJF) NAOI, positive

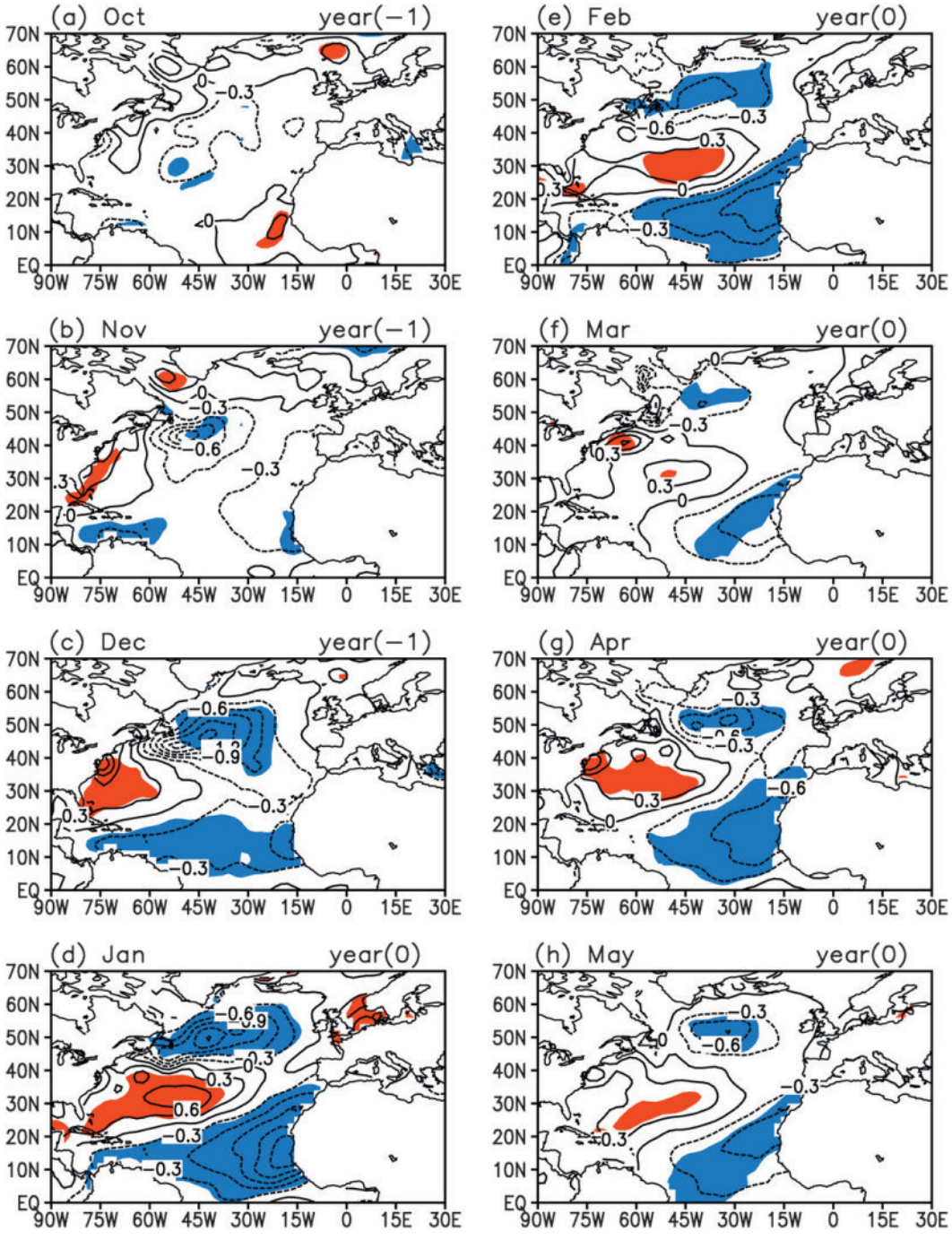

FIG. 10. Composite SSTA difference between positive and negative NAO cases (positive minus negative). Contour interval is 0.3°C; anomalies significant at the 95% level are shaded.

(index ≥ 1 SD) and negative (index ≤ −1 SD) NAO cases are selected. The year assigned to each winter is the one including January and February, as with the year assigned to strong ENSO cases. The positive cases include the winters of 1952, 1957, 1983, 1986, 1987, 1989, 1994, 1999, and 2001 while the negative cases include the winters of 1953, 1956, 1958, 1963, 1967, 1969, 1970, 1982, and 1996. Figure 10 shows the composite difference patterns of the SSTA between the positive and negative (i.e., positive minus negative) NAO cases. The tripolelike SSTA pattern occurs in the North Atlantic during winter, during which time the NTA region is dominated by

negative SSTA. The tripolelike SSTA pattern persists from winter through spring, meaning that the NTA SSTA associated with NAO does not experience a persistence barrier during winter. In contrast, it shows good persistence for the starting months of December and January. Therefore, in terms of the evolution of the NTA SSTA associated with the NAO, it appears that the NAO enhances persistence of the NTA SSTA during winter, which is unfavorable for the occurrence of the WPB.

However, because ENSO has greater influence in the tropics and subtropics, whereas the NAO dominates the midhigh latitudes (Kushnir et al. 2006), the NAO influence on the persistence of the NTA SSTA is generally small. After the NAO signal is linearly removed from the original NTA SSTA, the persistence of the residual NTA SSTA only shows little differences with that of the original NTA SSTA (Figs. 11a,b). Autocorrelations starting from November to February are reduced by more than 0.1 for lag times of 1–4 months after the NAO signal is removed (Fig. 11b), indicating that NAO can enhance the persistence of the NTA SSTA during winter. This result is consistent with that inferred from Fig. 10. During strong ENSO events, NTA variability is dominated by ENSO, leading to a prominent WPB. During weak ENSO or non-ENSO events, it is possible that the NAO plays an important role in determining the persistence of NTA SSTAs during winter, resulting in an indiscernible WPB.

The NAO shows similar seasonality to ENSO, both of which are strongest during winter (Rasmusson and Carpenter 1982; Hurrell 1995). However, it is important to ask why NAO does not produce a WPB in the NTA. One possible reason is that the NTA SSTA responds more quickly to NAO than to ENSO. As mentioned above, the Pacific ENSO usually induces a response in the NTA region with a lag of approximately 3–5 months; consequently, the NTA SSTA due to ENSO attains a maximum in spring (March–May). A sign reversal of the NTA SSTA occurs during winter, thereby resulting in a persistence barrier. In contrast, the NAO leads the North Atlantic SSTA by about 1 month. When strong NAO events occur during boreal winter, the tripolelike SSTA pattern driven by the NAO occurs in the North Atlantic at this time. The tripolelike SSTA pattern could persist from winter through spring, tending to enhance the persistence of the NTA SSTA during winter.

Another possible reason (for why the NAO does not produce a WPB in the NTA) is that the NTA SSTA has a QBO relationship with ENSO but not with the NAO. Huang (2004) finds that the ENSO influence on the tropical Atlantic Ocean is present throughout the year but has distinct seasonal characteristics. As shown in Fig. 9a, the NTA SSTA has a strong lead–lag correlation

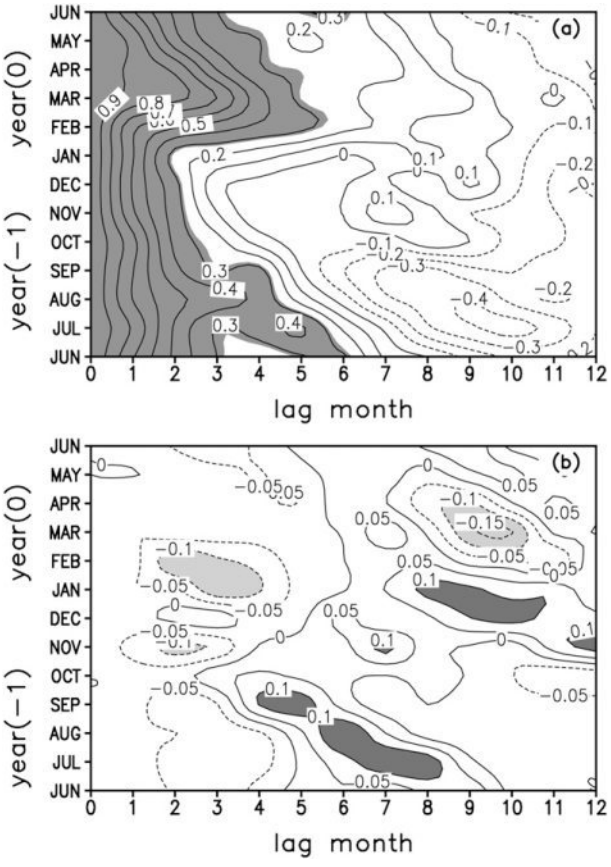

FIG. 11. (a) As in Fig. 1a, but for the residual NTA SSTA obtained by removing the NAO signal from the original NTA SSTA. The lead–lag correlations with the NAOI show that the NTA SSTA has significant correlations with the NAOI with lag times of 1–2 months. Therefore, the NAO signal in the NTA SSTA is obtained by regressing the NTA SSTA upon the NAO with lag times of 1–2 months. (b) As in Fig. 4, but for the difference between autocorrelations obtained from the residual NTA SSTA (as shown in Fig. 11a) and those obtained from the original NTA SSTA (as shown in Fig. 1a).

with ENSO throughout the year, except during winter months (December and January) when the NTA SSTA shows a sign reversal. The NAO, in contrast, is more likely to be associated with the relatively chaotic atmospheric internal variations and is probably less persistent on seasonal and longer time scales. The NAO influence on NTA SSTAs is mainly confined to winter and spring. The NTA SSTA shows a strong correlation with NAO during winter and spring, but it shows weak correlations during summer and autumn (Fig. 9b). The QBO relationship between the NTA SSTA and NAO does not exist; consequently, the NTA SSTA does not show a sign reversal during December and January associated with NAO. As a result of all these factors, the NTA WPB results primarily from ENSO, not NAO.

7. Summary and discussion

This study investigated the persistence characteristics of the SST anomaly (SSTA) in the northern tropical Atlantic (NTA). Autocorrelations of the NTA SSTA (area mean of the domain 5°–15°N, 20°–60°W) for the period 1950−2002 show a rapid decrease in December–January, regardless of the starting month, revealing the existence of a winter persistence barrier (WPB) in the NTA SST. The NTA WPB is prominent during the mature phase of strong ENSO cases but becomes indistinct in the weak ENSO and normal (i.e., non-ENSO) cases, indicating a close connection between the NTA WPB and ENSO. During strong El Niño cases, the NTA SSTA experiences a reversal in sign and rapid warming during winter. This SSTA sign reversal may reduce the persistence, creating favorable conditions for the occurrence of the NTA WPB. The NTA SSTA undergoes a sign reversal between the periods before and after the occurrence of the WPB, which implicates a possible connection between the WPB and the quasi-biennial oscillation (QBO) of the NTA SST. There may be a dynamic relationship among the Pacific ENSO, the NTA SSTA, and the NTA WPB on the quasi-biennial time scale as follows: a strong El Niño event is usually preceded by a strong La Niña event, which leads to a sign reversal of the NTA SSTA in winter as a delayed response to ENSO, ultimately resulting in the NTA WPB. During weak ENSO and normal cases, the NTA SSTA shows weak intensity and no phase reversal in winter; and the WPB of the NTA SST becomes indiscernible in these cases.

Because the atmospheric circulation and heat flux anomalies related to the North Atlantic Oscillation (NAO) modulate the SSTA over the NTA area, the NTA WPB also tends to be affected by the NAO. The present results show that NAO events are able to enhance the persistence of the NTA SSTA during winter, thereby weakening the NTA WPB. However, because ENSO has greater influence in the tropics and subtropics, whereas the NAO dominates the midhigh latitudes, the NAO tends to weaken (but not completely eliminate) the NTA WPB.

In addition to remote forcing of ENSO and the NAO, regional ocean–atmosphere interaction is a dominant factor affecting climate variability in the NTA. Regional ocean–atmosphere interaction includes a positive thermodynamic feedback among the surface trade wind, evaporation, and SST (WES) (Chang et al. 1997; Xie 1999) and dynamic feedback among the zonal wind, oceanic thermocline, and SST along the equator (Zebiak 1993). Recent studies have suggested that regional ocean–atmosphere interaction can be effective in producing anomalous SST fluctuations in the tropical Atlantic Ocean. Huang et al. (2002) noted that the SSTA in the NTA is strongly affected by the Pacific ENSO with local coupling accounting for an enhanced effect. Chang et al. (1998) investigated the predictability of SST in the NTA region, reporting a short lead time for predictability related to ENSO and enhanced predictability due to regional ocean–atmosphere interactions within the tropical Atlantic. Huang and Shukla (2005) found that the NTA SSTA is likely to persist within the subtropics for more than one season after it is generated, possibly caused by a local positive feedback between SST anomalies and the atmospheric anticyclone in the subtropics.

The above findings lead us to speculate that regional ocean–atmosphere interaction may have a strong influence on the persistence of the NTA SST. The evolutions of the NTA SSTA are driven by several mechanisms with comparable influences, involving both regional ocean–atmosphere interaction and remote forcings. These mechanisms may be seasonally dependent, which in turn determines the seasonal variations of SST persistence. Because it is difficult to isolate the individual influence of various mechanisms on SST persistence in the NTA region, further study is required using a coupling ocean–atmosphere general circulation model (CGCM).

Huang (2004) and Bates (2008, 2010) showed that the tropical Atlantic variability is composed of three major patterns: the southern tropical Atlantic (STA) pattern with SST variability expanding from the Angola coast to the central equatorial Atlantic and the Gulf of Guinea, the northern tropical Atlantic (NTA) pattern centered near the northern African coast, and the southern subtropical Atlantic (SSA) pattern in the open subtropical Atlantic. This study identifies a WPB associated with ENSO in the NTA. However, ENSO has been shown to affect SST in all regions of the tropical Atlantic, including the STA and the SSA (Enfield and Mayer 1997; Saravanan and Chang 2000; Elliott et al. 2001; Mo and Häkkinen 2001; Huang 2004; Bates 2008, 2010). Warming in the Gulf of Guinea has been shown to be related to ENSO warming (Horel et al. 1986; Carton and Huang 1994; Latif and Barnett 1995; Latif and Grötzner 2000). The connection between ENSO and SSA is thought to occur via a Pacific–South American (PSA) pattern (Mo and Higgins 1998; Bates 2010). Apart from ENSO, the SSA region is also affected by extratropical fluctuations (Bates 2010), such as the southern annular mode (SAM) (Gong and Wang 1999). The remote forcings of ENSO and SAM show seasonal influences on the SSA. Ciasto and Thompson (2008) found the influence in the South Atlantic to be mainly from ENSO in austral winter and SAM in austral summer. The mechanisms driving the SST fluctuations in the STA are similar to those in the NTA. However, the ENSO connection is thought to be weaker over the South Atlantic than over the North Atlantic (Enfield and Mayer

1997; Klein et al. 1999; Huang et al. 2004; Xie and Carton 2004). Bates (2008) showed that SSTA in the NTA region is related to a weakening of the northeast trade winds and that the wind stress anomalies act to enhance and maintain the NTA variability through the WES mechanism, which can lead to variability in the STA region through the influence of cross-equatorial winds. From the findings of Bates we can conclude that the SST persistence in the STA may be related to SST persistence in the NTA. A more thorough study of SST persistence remains to be done for the South Atlantic at a later date.

Another important point to be considered is the influence of the WPB on predictions of the NTA SSTA. It is well known that the spring persistence barrier (SPB) results in a decrease in forecast skill for most ENSO forecast models during boreal spring (March–May). If predictions are made across the boreal winter, it is highly likely that the NTA SSTA affected by the WPB has a low forecast skill. However, considering the delayed response of the NTA region to ENSO, the winter ENSO SST may be used to predict the ensuing spring and summer NTA SSTA. We speculate that, if strong El Niño events could be successfully predicted, warming in the NTA would be expected and the influence of the WPB on predictions of the NTA SSTA would be reduced. Further study is required to verify this speculation and to perform a concrete analysis of the influence of the WPB on predictions of the NTA SSTA.

Acknowledgments. We wish to thank two anonymous reviewers for helpful comments and suggestions, which helped to substantially improve the quality of this paper. This research was funded by an NSFC Project (40805022) and the 973 program (2010CB950400).

REFERENCES

An, S. I., and B. Wang, 2001: Mechanisms of locking the El Niño and La Niña mature phases to boreal winter. *J. Climate,* **14,** 2164–2176.

Barnston, A. G., M. H. Glanz, and Y. He, 1999: Predictive skill of statistical and dynamical climate models in forecasts of SST during the 1997–98 El Niño episode and the 1998 La Niña onset. *Bull. Amer. Meteor. Soc.,* **80,** 217–243.

Bates, S. C., 2008: Coupled ocean–atmosphere interaction and variability in the tropical Atlantic Ocean with and without an annual cycle. *J. Climate,* **21,** 5501–5523.

——, 2010: Seasonal influences on coupled ocean–atmosphere variability in the tropical Atlantic Ocean. *J. Climate,* **23,** 582–604.

Bjerknes, J., 1969: Atmospheric teleconnections from the equatorial Pacific. *Mon. Wea. Rev.,* **97,** 163–172.

Blumenthal, M. B., 1991: Predictability of a coupled ocean–atmosphere model. *J. Climate,* **4,** 766–784.

Carton, J. A., and B. Huang, 1994: Warm events in the tropical Atlantic. *J. Phys. Oceanogr.,* **24,** 888–903.

——, X. H. Cao, B. S. Giese, and A. M. da Silva, 1996: Decadal and interannual SST variability in the tropical Atlantic ocean. *J. Phys. Oceanogr.,* **26,** 1165–1175.

Chang, P., L. Ji, and H. Li, 1997: A decadal climate variation in the tropical Atlantic Ocean from thermodynamic air-sea interactions. *Nature,* **385,** 516–518.

——, ——, ——, C. Penland, and L. Matrosova, 1998: Prediction of tropical Atlantic sea surface temperature. *Geophys. Res. Lett.,* **25,** 1193–1196.

——, R. Saravanan, and L. Ji, 2003: Tropical Atlantic seasonal predictability: The roles of El Niño remote influence and thermodynamic air-sea feedback. *Geophys. Res. Lett.,* **30,** 1501, doi:10.1029/2002GL016119.

——, and Coauthors, 2006: Climate fluctuations of tropical coupled system—The role of ocean dynamics. *J. Climate,* **19,** 5122–5174.

Chen, J.-M., L. Tim, and C.-F. Shih, 2007: Fall persistence barrier of sea surface temperature in the South China Sea associated with ENSO. *J. Climate,* **20,** 158–172.

Ciasto, L. M., and D. W. Thompson, 2008: Observations of large-scale ocean–atmosphere interaction in the Southern Hemisphere. *J. Climate,* **21,** 1244–1259.

Clarke, A. J., and S. Van Gorder, 1999: The correlation between the boreal spring Southern Oscillation persistence barrier and biennial variability. *J. Climate,* **12,** 610–620.

Czaja, A., P. van der Varrt, and J. Marshall, 2002: A diagnostic study of the role of remote forcing in tropical Atlantic variability. *J. Climate,* **15,** 3280–3290.

Deser, C., and M. Timlin, 1997: Atmosphere–ocean interaction on weekly timescales in the North Atlantic and Pacific. *J. Climate,* **10,** 393–408.

——, M. A. Alexander, and M. S. Timlin, 2003: Understanding the persistence of sea surface temperature anomalies in midlatitudes. *J. Climate,* **16,** 57–72.

Ding, R. Q., and J. P. Li, 2009: Decadal and seasonal dependence of North Pacific SST persistence. *J. Geophys. Res.,* **114,** D01105, doi:10.1029/2008JD010723.

Elliott, J., S. P. Jewson, and R. T. Sutton, 2001: The impact of the 1997/98 El Niño events on the Atlantic Ocean. *J. Climate,* **14,** 1069–1077.

Enfield, D. B., 1996: Relationships of inter-American rainfall to tropical Atlantic and Pacific SST variability. *Geophys. Res. Lett.,* **23,** 3305–3308.

——, and D. A. Mayer, 1997: Tropical Atlantic sea surface temperature variability and its relation to El Niño–Southern Oscillation. *J. Geophys. Res.,* **102,** 929–945.

Folland, C. K., T. N. Palmer, and D. E. Parker, 1986: Sahel rainfall and worldwide sea temperatures, 1901–85. *Nature,* **320,** 602–607.

Foltz, G. R., and M. J. McPhaden, 2006: The role of oceanic heat advection in the evolution of tropical north and south Atlantic SST anomalies. *J. Climate,* **19,** 6122–6138.

Giannini, A., J. C. H. Chiang, M. A. Cane, Y. Kushnir, and R. Seager, 2001a: The ENSO teleconnection to the tropical Atlantic Ocean: Contributions of the remote and local SSTs to rainfall variability in the tropical Americas. *J. Climate,* **14,** 4530–4544.

——, M. A. Cane, and Y. Kushnir, 2001b: Interdecadal changes in the ENSO teleconnection to the Caribbean region and the North Atlantic Oscillation. *J. Climate,* **14,** 2867–2879.

Gong, D., and S. Wang, 1999: Definition of Antarctic oscillation index. *Geophys. Res. Lett.,* **26,** 459–462.

Goswami, B. N., and J. Shukla, 1991: Predictability of a coupled ocean–atmosphere model. *J. Climate,* **4,** 3–22.

Grötzner, A., M. Latif, and T. P. Barnett, 1998: A decadal climate cycle in the North Atlantic Ocean as simulated by the ECHO coupled GCM. *J. Climate,* **11,** 831–847.

Handoh, I. C., A. J. Matthews, G. R. Bigg, and D. P. Stevens, 2006: Interannual variability of the tropical Atlantic independent of

and associated with ENSO: Part I. The North Tropical Atlantic. *Int. J. Climatol.,* **26,** 1937–1956.

Horel, J. D., V. E. Kousky, and M. T. Kagaro, 1986: Atmospheric conditions in the tropical Atlantic during 1983–1984. *Nature,* **322,** 243–245.

Huang, B., 2004: Remotely forced variability in the tropical Atlantic Ocean. *Climate Dyn.,* **23,** 133–152.

——, and J. Shukla, 2005: Ocean–atmosphere interactions in the tropical and subtropical Atlantic Ocean. *J. Climate,* **18,** 1652–1672.

——, P. S. Schopf, and Z. Q. Pan, 2002: The ENSO effect on the tropical Atlantic variability: A regionally coupled model study. *Geophys. Res. Lett.,* **29,** doi:10.1029/2002GL014872.

——, ——, and J. Shukla, 2004: Intrinsic ocean–atmosphere variability of the tropical Atlantic ocean. *J. Climate,* **17,** 2058–2077.

Hurrell, J. W., 1995: Decadal trends in the North Atlantic Oscillation: Regional temperatures and precipitation. *Science,* **269,** 676–679.

Jin, E. K., and Coauthors, 2008: Current status of ENSO prediction skill in coupled ocean-atmosphere models. *Climate Dyn.,* **31,** 647–664.

Kalnay, E., and Coauthors, 1996: The NCEP–NCAR 40-Year Reanalysis Project. *Bull. Amer. Meteor. Soc.,* **77,** 437–471.

Klein, S. A., B. J. Soden, and N.-C. Lau, 1999: Remote sea surface temperature variations during ENSO: Evidence for a tropical atmospheric bridge. *J. Climate,* **12,** 917–932.

Kushnir, Y., W. A. Robinson, P. Chang, and A. W. Robertson, 2006: The physical basis for predicting Atlantic sector seasonal-to-interannual climate variability. *J. Climate,* **19,** 5949–5970.

Latif, M., and T. P. Barnett, 1995: Interactions of the tropical oceans. *J. Climate,* **8,** 952–968.

——, and A. Grötzner, 2000: The equatorial Atlantic oscillation and its response to ENSO. *Climate Dyn.,* **16,** 213–218.

——, and Coauthors, 1998: A review of the predictability and prediction of ENSO. *J. Geophys. Res.,* **103,** 14 375–14 393.

Li, J., and J. Wang, 2003: A new North Atlantic Oscillation index and its variability. *Adv. Atmos. Sci.,* **20,** 661–676.

Luo, J. J., S. Masson, S. Behera, and T. Yamagata, 2007: Experimental forecasts of Indian Ocean dipole using a coupled OAGCM. *J. Climate,* **20,** 2178–2190.

Marshall, J., and Coauthors, 2001: North Atlantic climate variability: Phenomena, impacts, and mechanisms. *Int. J. Climatol.,* **21,** 1863–1898.

Mo, K. C., and R. W. Higgins, 1998: The Pacific–South American modes and tropical convection during the Southern Hemisphere winter. *Mon. Wea. Rev.,* **126,** 1581–1596.

——, and S. Häkkinen, 2001: Interannual variability in the tropical Atlantic and linkages to the Pacific. *J. Climate,* **14,** 2740–2762.

Moura, A. D., and J. Shukla, 1981: On the dynamics of droughts in northeast Brazil: Observations, theory, and numerical experiments with a general circulation model. *J. Atmos. Sci.,* **38,** 2653–2675.

Namias, J., and R. M. Born, 1970: Temporal coherence in North Pacific sea surface temperature patterns. *J. Geophys. Res.,* **75,** 5952–5955.

——, and ——, 1974: Further studies of temporal coherence in North Pacific sea surface temperature patterns. *J. Geophys. Res.,* **79,** 797–798.

Nobre, P., and J. Shukla, 1996: Variations of sea surface temperature, wind stress, and rainfall over the tropical Atlantic and South America. *J. Climate,* **9,** 2464–2479.

Oort, A. H., and E. M. Rasmusson, 1970: On the annual variation of the monthly mean meridional circulation. *Mon. Wea. Rev.,* **98,** 423–442.

Pan, L., 2005: Observed positive feedback between the NAO and the North Atlantic SSTA tripole. *Geophys. Res. Lett.,* **32,** L06707, doi:10.1029/2005GL022427.

Penland, C., and L. Matrosova, 1998: Prediction of tropical Atlantic sea surface temperatures using linear inverse modeling. *J. Climate,* **11,** 483–496.

Rasmusson, E. M., and T. H. Carpenter, 1982: Variations in tropical sea surface temperature and surface wind fields associated with the Southern Oscillation–El Niño. *Mon. Wea. Rev.,* **110,** 354–384.

——, X. Wang, and C. F. Ropelewski, 1990: The biennial component of ENSO variability. *J. Mar. Syst.,* **1,** 71–96.

Saji, N. H., B. N. Goswami, P. N. Vinayachandran, and T. Yamagata, 1999: A dipole mode in the tropical Indian Ocean. *Nature,* **401,** 360–363.

Saravanan, R., and P. Chang, 2000: Interaction between tropical Atlantic variability and El Niño–Southern Oscillation. *J. Climate,* **13,** 2177–2194.

Smith, T. M., and R. W. Reynolds, 2004: Improved extended reconstruction of SST (1854–1997). *J. Climate,* **17,** 2466–2477.

Sutton, R. T., S. P. Jewson, and D. P. Rowell, 2000: The elements of climate variability in the tropical Atlantic region. *J. Climate,* **13,** 3261–3284.

Taschetto, A. S., and I. Wainer, 2008: The impact of the subtropical South Atlantic SST on South American precipitation. *Ann. Geophys.,* **26,** 3457–3476.

Torrence, C., and P. J. Webster, 1998: The annual cycle of persistence in the El Niño–Southern Oscillation. *Quart. J. Roy. Meteor. Soc.,* **124,** 1985–2004.

Wajsowicz, R. C., 2005: Potential predictability of tropical Indian Ocean SST anomalies. *Geophys. Res. Lett.,* **32,** L24702, doi:10.1029/2005GL024169.

Wallace, J. M., and D. S. Gutzler, 1981: Teleconnections in the geopotential height field during the Northern Hemisphere winter. *Mon. Wea. Rev.,* **109,** 784–812.

Wang, C., 2002: Atlantic climate variability and its associated atmospheric cells. *J. Climate,* **15,** 1516–1536.

——, 2004: ENSO, Atlantic climate variability, and the Walker and Hadley circulations. *The Hadley Circulation: Past, Present and Future,* H. F. Diaz and R. S. Bradley, Eds., Advances in Global Change Research, Vol. 21, Kluwer Academic Publishers, 85–120.

Webster, P. J., and S. Yang, 1992: Monsoon and ENSO: Selectively interactive systems. *Quart. J. Roy. Meteor. Soc.,* **118,** 877–925.

Xie, S.-P., 1999: A dynamic ocean–atmosphere model of the tropical Atlantic decadal variability. *J. Climate,* **12,** 64–70.

——, and J. A. Carton, 2004: Tropical Atlantic variability: Patterns, mechanisms, and impacts. *Earth Climate: The Ocean–Atmosphere Interaction,* C. Wang, et al., Eds., *Geophys. Monorgr.,* No. 147, Amer. Geophys. Union, 121–142.

Yu, J. Y., 2005: Enhancement of ENSO's persistence barrier by biennial variability in a coupled atmosphere-ocean general circulation model. *J. Geophys. Res.,* **32,** L13707, doi:10.1029/2005GL023406.

Zebiak, S. E., 1993: Air–sea interaction in the equatorial Atlantic region. *J. Climate,* **6,** 1567–1586.

——, and M. A. Cane, 1987: A model El Niño–Southern Oscillation. *Mon. Wea. Rev.,* **115,** 2262–2278.

Zhao, X., and J. P. Li, 2009: Possible causes for the persistence barrier of SSTA in the South China Sea and the vicinity of Indonesia. *Adv. Atmos. Sci.,* **26,** 1125–1136.

——, and ——, 2010: Winter-to-winter recurrence of sea surface temperature anomalies in the Northern Hemisphere. *J. Climate,* **23,** 3835–3854.